

# Low-loss coupling technique between SOI waveguides and standard single-mode fibers

J. V. Galán (1), P. Sanchis (2) and J. Martí (3)

Valencia Nanophotonics Technology Center, 1) jogaco@ntc.upv.es, 2) pabsanki@ntc.upv.es, 3) jmarti@ntc.upv.es

**Abstract:** In this paper, an inverted taper-based technique for highly efficient coupling between SOI waveguides and standard single-mode fibers is reported. The coupling structure is polarization insensitive and it is based on the inverted taper coupled to a fiber-adapted waveguide. In this case, the fiber-adapted waveguide is made by using the SiO<sub>2</sub> layer under the Si waveguiding layer of the SOI wafer thus avoiding the use of extra materials such as polymers. The proposed coupling structure is aimed for being integrated with V-groove auto-alignment techniques. Coupling losses of 4.21dB and 4.5dB to 10 $\mu$ m mode field diameter standard single-mode fibers have been estimated for TE and TM polarizations respectively and 1550nm performance.

## Introduction

Efficient coupling between standard single-mode fibers and single-mode waveguides is a key point in silicon photonics. An optical integrated circuit is useless without an interface to the outside world. The small size of single-mode silicon-on-insulator (SOI) waveguides (typically 500nm width and around 200nm thickness) compared with the high diameter of a single-mode fiber (between 8-10 $\mu$ m) makes coupling inefficient. A direct end-fire coupling between a SOI single-mode waveguide and a standard single-mode optical fiber means around 20dB of coupling losses for TE polarization and 1550nm input signal wavelength. Three-dimensional (3D) tapers have been reported to achieve 3D spot-size conversion between the spot-sizes of the waveguide and the fiber [1]. More complex structures such as two different tapers formed at different levels have also been proposed [2]. However, the complexity of the fabrication significantly increases in 3D approaches and the coupling length is typically higher than 500 $\mu$ m. A more elegant and compact solution that is compatible with planar processing techniques is the use of two-dimensional (2D) inverted tapers to achieve 3D spot-size conversion [3-9]. In this case, the width of the taper is gradually decreased thus delocalizing the mode profile out of the waveguide core.

The tip of the inverted taper can be directly attached to the optical fiber [4,5]. However, in this case, very precise control on the chip facets position is required. Therefore, the mode out of the inverted taper is usually coupled into another fiber-adapted waveguide. This fiber-adapted waveguide is made of low index contrast polymer materials and it is placed on top of the inverted taper [6-9]. However, the inverted taper and the low-index contrast waveguide are optimized for low coupling losses into small core optical fibers

with typically 3-4  $\mu$ m mode field diameter (MFD). In this paper, a new coupling structure based on the inverted taper is proposed for low coupling losses between SOI waveguides and standard single-mode fibers with 10 $\mu$ m MFD. The proposed approach is polarization insensitive and it takes advantage of the SiO<sub>2</sub> layer under the Si waveguiding layer of the SOI wafer to obtain the fiber-adapted waveguide. Furthermore, the structure is designed with the aim of future integration with V-groove structures thus allowing passive alignment and easier packaging [10].

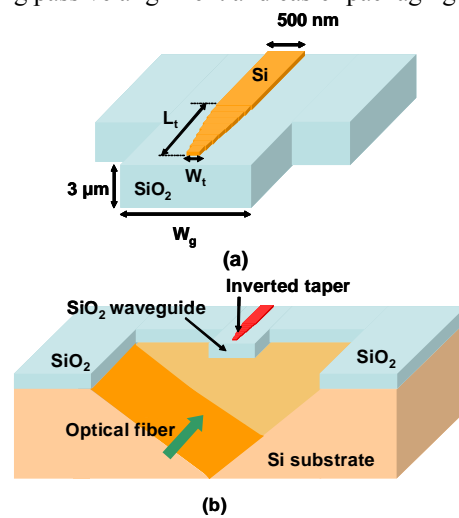


**Fig. 1:** (a) Proposed inverted taper-based structure and its main design parameters. (b) Detail of the integration of the proposed structure with the V-groove auto-alignment structure.

## Proposed structure

The proposed inverted taper-based structure is shown in Fig. 1(a). The single-mode SOI waveguide is tapered down by the inverted taper. As SOI wafers of 205nm/3 $\mu$ m Si/SiO<sub>2</sub> layer thicknesses have been used, the Si waveguide width has to be around 500nm to achieve single-mode propagation. The main inverted taper design parameters are the inverted taper length ( $L_t$ ) and the inverted taper tip width ( $W_t$ ) both illustrated in Fig. 1(a). If the substrate of the SOI wafer is removed, it is possible to use the SiO<sub>2</sub> layer as the fiber-adapted waveguide, as shown in Fig. 1(a). Due to the SiO<sub>2</sub> SOI wafer layer thickness, the height of the SiO<sub>2</sub> waveguide is fixed to 3 $\mu$ m. The objective is to find the optimum SiO<sub>2</sub> waveguide width and the optimum inverted taper parameters to achieve the lowest coupling losses between the proposed structure and the standard single-mode fiber. Furthermore, the design is carried out to obtain a polarization insensitive structure. The most important application of the proposed structure is its

direct integration with V-groove auto-alignment structures as illustrated in Fig. 1(b). A step by step analysis of the proposed inverted taper-based structure is presented on the following sections. The analysis starts with the SiO<sub>2</sub> waveguide section parameters design in the fiber-SiO<sub>2</sub> waveguide interface to achieve the highest coupling efficiency to 10 $\mu$ m MFD standard single-mode fibers. Then, the optimum inverted taper tip width and length are designed.

### SiO<sub>2</sub> waveguide width design

To find the optimum SiO<sub>2</sub> waveguide width to get the highest coupling efficiency between the SiO<sub>2</sub> waveguide and the fiber, a 3D overlap integral between fiber and waveguide fundamental mode profiles has been used. The fundamental mode profile of the SiO<sub>2</sub> waveguide has been obtained by a 3D mode solver based on the Beam Propagation Method (BPM). The fundamental mode profile of the fiber has been approximated by a Gaussian beam as a function of the fiber mode field diameter. The simulation results are shown in Fig. 2. The figure shows the estimated coupling efficiency between the SiO<sub>2</sub> waveguide and the fiber as a function of the fiber mode field diameter for different SiO<sub>2</sub> waveguide widths and a 1550nm input signal wavelength. A polarization insensitive behaviour of the coupling efficiency in the SiO<sub>2</sub> waveguide-fiber interface was observed, so results shown in Fig. 2 are valid for both TE and TM polarizations. As it is shown in Fig. 2, the estimated coupling losses for an 8 $\mu$ m width SiO<sub>2</sub> waveguide and a standard single-mode fiber (10 $\mu$ m mode field diameter) are around 4.2dB for both TE and TM polarizations and a 1550nm input signal wavelength. If the waveguide gets wider (e.g. 10 $\mu$ m width), the estimated coupling losses are only 0.4dB less than in the 8 $\mu$ m width SiO<sub>2</sub> waveguide case. Therefore, in order to minimize as much as possible the SiO<sub>2</sub> waveguide dimensions, the 8 $\mu$ m width SiO<sub>2</sub> waveguide case has been considered for the next inverted taper design parameters simulations.

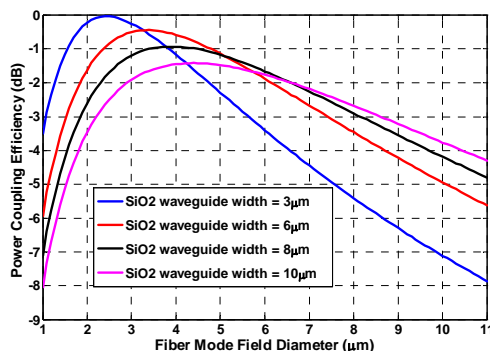


**Fig. 2:** Power coupling efficiency between the SiO<sub>2</sub> waveguide and the optical fiber as function of the fiber mode field diameter for different waveguide widths,  $\lambda=1550$ nm and both TE and TM polarizations.

### Inverted taper tip width design

In order to find the optimum tip width of the inverted taper, it has been considered the inverted taper tip-SiO<sub>2</sub> waveguide interface of the proposed structure. It is possible to obtain the fundamental mode profiles of both the fiber-adapted SiO<sub>2</sub> waveguide with and without the inverted taper on top. These fundamental mode profiles have been obtained by a 3D mode solver based on the Beam Propagation Method (BPM). Evaluating the overlap integral of both fundamental mode profiles for different inverted taper tip widths, the final inverted taper tip width has been chosen the optimal one that results in the highest power coupling efficiency of the mentioned interface.

The simulation results are shown in Fig. 3. The figure shows the estimated coupling efficiency between the SiO<sub>2</sub> waveguide with and without the inverted taper tip on top, as a function of the inverted taper tip width for a 1550nm input signal wavelength and for both TE and TM polarizations. According to Fig. 3, almost negligible coupling losses are achieved in the taper tip interface for inverted taper tip widths lower than 200nm and for both TE and TM polarizations (around 0.01dB coupling losses for TE polarization and 0.3dB for TM polarization). Therefore, if a lower than 200nm inverted taper tip width is chosen, the proposed design is polarization insensitive in the considered interface. In order to maximize as much as possible the inverted taper tip width for an easier future fabrication, the 200 nm inverted taper tip width case has been chosen.

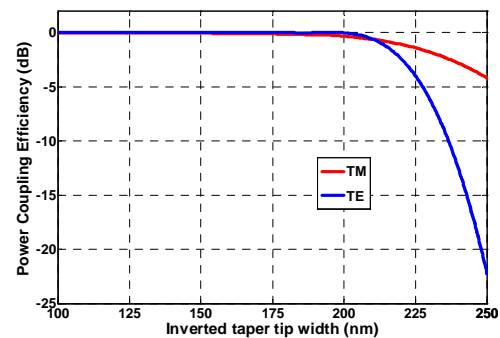


**Fig. 3:** Power coupling efficiency between the SiO<sub>2</sub> waveguide with and without the inverted taper on the top, respectively, according to Fig. 3(b) as a function of the inverted taper tip width,  $\lambda=1550$ nm and for both TE and TM polarizations.

### Inverted taper length design

The optimum inverted taper length has been designed by means of FDTD simulations using the inverted taper tip width ( $W_t=200$ nm) and the SiO<sub>2</sub> waveguide width ( $W_g=8\mu$ m) that were found to be the optimum ones in the previous sections. 3D FDTD simulations require very high computational memory because of the relative large taper length. So, the taper length effect has been simulated using 2D FDTD simulations. To take into account the neglected structure dimension in the 2D problem approximation, the

effective index method has been used. Two possibilities have been studied depending on the spatial perspective of the 2D structure approximation. It is possible to analyze the coupling structure according to a 2D top view or according to a 2D side view too. The used 2D FDTD simulations including these two 2D perspective views are shown in Fig. 4. In Fig. 4(a) the 2D top view FDTD structure simulation is illustrated while in Fig. 4(b) it is shown the 2D side view one. Basically, in the simulations in Fig. 4, the structure is excited by the SiO<sub>2</sub> slab waveguide fundamental mode at a 1550nm wavelength, and the Si waveguide coupled power is measured by a power monitor. As the schematics in Fig. 4 are being excited by the SiO<sub>2</sub> slab waveguide fundamental mode, the fiber-SiO<sub>2</sub> waveguide interface is not being considered. So, to obtain the total SOI waveguide-to-fiber coupling losses, the estimated coupling losses depending on the taper length have to be added to the estimated ones in the SiO<sub>2</sub> waveguide width design for the fiber-SiO<sub>2</sub> waveguide interface (4.2dB for a 10μm MFD standard single-mode fiber and both TE and TM polarizations).

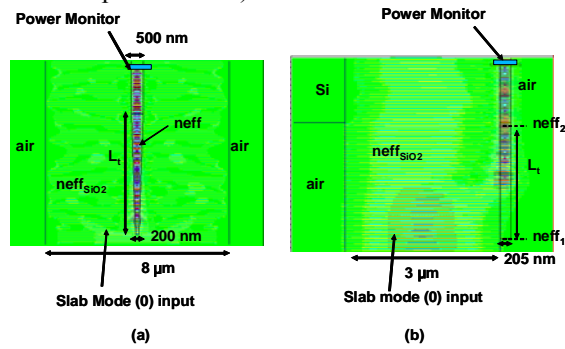


**Fig. 4:** Detail of the carried out 2D FDTD simulation to obtain the optimum inverted taper length. The effective index method has been used in both (a) 2D top view structure simulation, and (b) 2D side view structure simulation.

According to the 2D top view simulation in Fig. 4(a) and using the effective index method, the SiO<sub>2</sub> waveguide refractive index is replaced by an effective index ( $neff_{SiO_2}$  in Fig. 4(a) for both TE and TM polarizations) to consider the 3μm thickness of the SiO<sub>2</sub> waveguide. In the same way, the Si waveguide and taper refractive index is replaced by other effective index ( $neff$  in Fig. 4(a)), considering the 205nm Si layer thickness. For the 2D side view simulation in Fig. 4(b), a similar procedure has been carried out. The SiO<sub>2</sub> waveguide refractive index is replaced by an effective index to consider the 8μm width of that SiO<sub>2</sub> waveguide ( $neff_{SiO_2}$  in Fig. 4(b)). About the inverted taper effective index, as the taper width is not constant along the propagation direction, and remembering that the structure is being analyzed according to its 2D side view, the linear variation of the taper width along the propagation direction is now transformed in an effective index linear variation as a function of the inverted taper width. At the 200nm width inverted taper tip, the effective index ( $neff_1$  in Fig. 4(b)) considers the inverted taper tip width. That

effective index increases along the propagation direction until the 500nm Si waveguide width corresponding effective index ( $neff_2$  in Fig. 4(b)). The simulation results of both, 2D side view and 2D top view are shown in Fig. 5(a) for TE and in Fig. 5(b) for TM polarizations and for a 1550nm input signal wavelength.

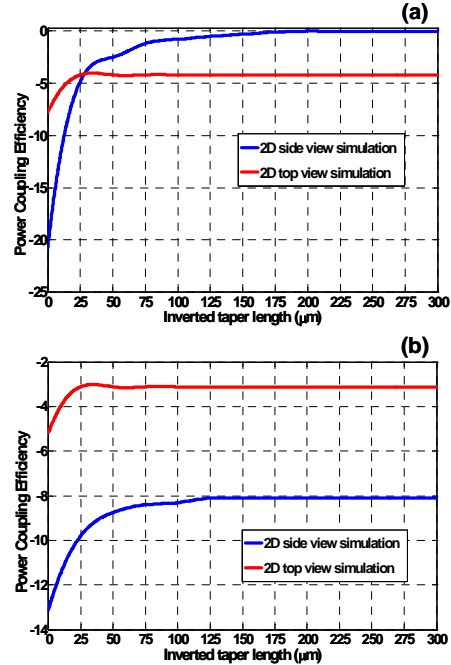


**Fig. 5:** Power coupling efficiency as a function of the inverted taper length for both 2D top and 2D side view FDTD simulations, 1550 nm input signal wavelength and for (a) TE and (b) TM polarizations.

Looking at Fig. 5(a) for TE polarization, it can be seen that the power coupling efficiency increases as the inverted taper gets longer due to the lower radiation losses. However, the 2D top view simulation in Fig. 5(a) does not behave just as the 2D side view one. In the 2D top view simulation, the obtained power coupling efficiency is maximum for a very low inverted taper length value which, in principle, does not seem realistic. Furthermore, in this case, it can be seen that the minimum coupling losses for the 2D top view simulation are not zero thus disagreeing with the 3D results shown in Fig. 3. This coupling losses value is due to the mode mismatch of the 2D approximation in the interface between the SiO<sub>2</sub> waveguide with and without the taper tip on top. 2D overlap integral between both the SiO<sub>2</sub> waveguide with and without the 200nm width taper tip on top confirmed the minimum coupling losses reached by the 2D FDTD simulations. For the 2D side view approximation, the minimum coupling losses calculated by the 2D overlap integral are very similar to the obtained value by means of the 3D overlap integral, which are around 0.01dB according to Fig. 3. So, it can be concluded that for TE polarization, the 2D side view simulation is a very good approximation of the 3D approach. The minimum inverted taper length to achieve negligible coupling losses is 200μm.

Taking a look in Fig. 5(b) for TM polarization, the same behavior than in the TE case is observed and the 2D side view simulation seems a better approximation than the 2D top view simulation. However, the minimum coupling losses obtained by means of the 2D side view simulation are not negligible. As for TE polarization, these coupling losses are due to the mode mismatch of the 2D approximation at the inverted taper tip-SiO<sub>2</sub> waveguide interface. Thereby, the 8dB minimum coupling losses were in agreement with the coupling losses obtained by means of a 2D overlap integral in the inverted taper tip-SiO<sub>2</sub> waveguide interface. So, these are the minimum coupling losses that the 2D approximation can reach according to the 2D side view simulation in Fig. 5(b). For a 125 $\mu$ m long inverted taper, the minimum coupling losses are reached and it corresponds to the mode mismatch in the inverted taper tip-SiO<sub>2</sub> waveguide interface, which were estimated in 0.3dB coupling losses by means of a 3D overlap integral according to Fig. 3 for TM polarization.

In order to have a similar behavior of the inverted taper for both TE and TM simulations, it has been chosen a 200 $\mu$ m long inverted taper. For a 200 $\mu$ m long inverted taper and for both TE and TM polarizations, the total SOI waveguide-to-fiber coupling losses are the sum of the fiber-SiO<sub>2</sub> waveguide interface coupling losses, which were estimated in 4.2dB, and the estimated coupling losses in the inverted taper tip-SiO<sub>2</sub> waveguide interface, which were estimated by means of the 3D overlap integral in 0.01dB and 0.3dB for TE and TM polarizations respectively, according to Fig. 3. It results in around 4.21dB and 4.5dB total coupling losses for TE and TM polarizations respectively.

### Spectral response

Having obtained the most important inverted taper design parameters for a standard single-mode fiber efficient coupling and a 1550 nm input signal wavelength, a spectral analysis of the proposed structure has been carried out. Fig. 6 shows the simulation results for the inverted taper-based structure spectral response taking into account a 10 $\mu$ m MFD standard single-mode fiber.

It is observed an almost flat spectral response of the proposed inverted taper-based structure in the considered wavelengths range for both TE and TM polarizations. Coupling losses can be reduced by using fibers with a lower core diameter, as it can be seen in Fig. 2.

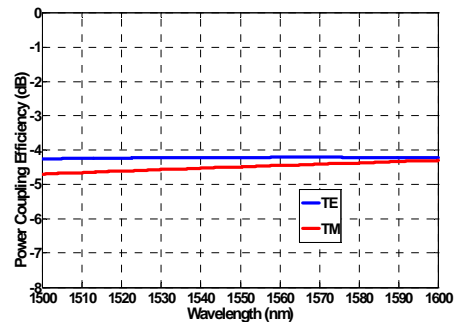


Fig. 6: Spectral response simulation results for the inverted taper-based structure and taking into account a 10 $\mu$ m MFD standard single-mode fiber.

### Conclusions

In this paper, we report a polarization insensitive fiber-to-SOI waveguide efficient coupling technique using an inverted taper-based structure. The SiO<sub>2</sub> layer of the SOI wafer is considered to make the fiber-adapted waveguide thus avoiding the use of extra materials such as polymers. The proposed coupling structure is aimed for being integrated with V-groove auto-alignment techniques. Parameters have been designed to maximize the coupling efficiency to standard single-mode fibers (MFD=10 $\mu$ m). Two different techniques based on the effective index method have been evaluated to simulate the inverted taper performance by means of 2D FDD simulations. It has been obtained that 2D side view approach is a better approximation than the 2D top view approach. Coupling losses of 4.21 dB and 4.5dB for TE and TM polarizations respectively and 1550 nm input signal wavelength have been obtained using a 200 $\mu$ m long inverted taper. Furthermore, a flat spectral response is achieved because the coupling structure performance does not rely on any resonant effect.

### Acknowledgments

Financial support by EC under project 017158-PHOLOGIC and Spanish MEC and EU-FEDER under contract TEC2005-07830 SILPHONICS is acknowledged. Authors also acknowledge financial support by Generalitat Valencia and Universidad Polit cnica de Valencia.

### References

- 1 A. Sure, et al, Opt. Express, 26, 3555-3561 (2003).
- 2 D. Dai, et al, IEEE JLT 24, 2418-2433 (2006).
- 3 T. Shoji, et al, EL, 38, 1669-1670 (2002).
- 4 L. Vivien, et al, IEEE JLT, 21, 1-5 (2003).
- 5 V. R. Almeida, et al, OL, 28, 1302-1304 (2003).
- 6 S. J. McNab, et al, OE, 11, 2927-2939 (2003).
- 7 K. Yamada, et al, IEICE TE, E87-C, 351-358 (2004).
- 8 K. K. Lee, et al, OL, 30, 498-500 (2005).
- 9 G. Roelkens, et al, PTL, 17, 2613-2615 (2005).
- 10 S. Park, et al, IEEE PTL, 17, 1444-1446 (2005).